Journal of Applied Polymer Science

# One pot blending of biopolymer-$TiO_2$ composite membranes with enhanced mechanical strength

**Zhonghua Huang,[1,2] Weijing Li,[1,2] Zhengli Liu,[1,2] Yan Zhang[1,2]**

[1]School of Environmental and Biological Engineering, Nanjing University of Science and Technology, Nanjing 210094, China
[2]Jiangsu Key Laboratory of Chemical Pollution Control and Resources Reuse, Nanjing University of Science and Technology, Nanjing 210094, China
Correspondence to: Z. Huang (E-mail: hzhlqfox@njust.edu.cn)

**ABSTRACT:** A biopolymer-$TiO_2$ composite membrane was prepared by blending of *N*-[(2-hydroxy-3-trimethylammonium) propyl] chloride chitosan and cellulose acetate with nano-$TiO_2$ particles as the introduced inorganic components. It was verified that the amino groups ($-NH_2$) of chitosan (CTS) were partly grafted by stronger hydrophilic group $-CH_2CH(OH)CH_2N(CH_3)_3^+$ according to the $^1$H-nuclear magnetic resonance spectra of *N*-[(2-hydroxy-3-trimethylammonium) propyl] chloride chitosan and attenuated total reflectance Fourier transform infrared spectroscopy. The structure, microcosmic morphology, water flux, swelling properties, and thermal stability of the composite membranes were characterized. With the mass ratio of cellulose acetate to CTS being 50 wt %, the mole ratio of CTS to glycidyl trimethylammonium chloride being 1 : 1, and drying temperature being 60°C in 70% acetic acid, the formed biopolymer-$TiO_2$ composite membranes exhibited enhanced mechanical strength (84.29 MPa), lower swelling degree (101.36%), and improved antibacterial activity against Gram-negative *Escherichia coli* (*Rosetta* and *DH5α*) and Gram-positive *Bacillus subtilis*. The existence of nano-$TiO_2$ particles and the introduction of stronger cationic group synergistically improved the antibacterial properties of the biopolymer-$TiO_2$ composite membranes.
 J. Appl. Polym. Sci. **2015**, *132*, 42732.

**KEYWORDS:** biopolymers; blends; mechanical properties; membranes; renewable polymers; synthesis and processing

Received 24 January 2015; accepted 12 July 2015
**DOI: 10.1002/app.42732**

## INTRODUCTION

Chitosan (CTS) is the *N*-deacetylated form of chitin, with repeating units of 2-acetamido-2-deoxy-β-D-glucopyranose. Because of its nontoxicity, biodegradability, hydrophilicity, unique polycationic nature, and good film-forming characteristics, CTS and its derivatives have been considered as a promising membrane biopolymer for pervaporation, ultrafiltration, reverse osmosis, gas separation, or purification processes.[1–5] However, the poor mechanical performance and swelling in aqueous solutions of the CTS membrane greatly restrict its application.[6] To improve the mechanical properties and control membrane swelling, much attention in CTS has been paid to the introduction of cross-linked structure to membrane,[7,8] blending of CTS with other polymers,[9] casting CTS solution on another membrane surface to form composite membranes,[10,11] and developing organic–inorganic composite membranes.[12–15]

Among the modification methods, polymer blending is simple and effective for providing satisfactory polymeric materials.[16–20] It is known that blending proves to be an efficient way to achieve combined properties of individual polymers.[21] Cellulose acetate (CA) is commonly used as membrane material because of its good toughness, high biocompatibility, moderate chlorine resistance, superior film-forming ability, and relatively low cost.[22–24] A key difference between CA and CTS is that the latter has an amino group instead of a hydroxyl group at C-2 of the glucopyranose ring. This similarity in primary structures suggests that the secondary structures and patterns of aggregation may also be sufficiently similar to facilitate the formation of homogeneous blends of the two polymers.[25–27] During the blended membrane formation, CA was chosen as the matrix polymer and CTS was used to introduce reactive sites (amino and hydroxyl groups) in the membrane materials. Therefore, additive or even synergistic effects can render the performance of CTS membrane more functional. For example, separation performance of the CA membrane can be increased by blending *N,O*-carboxymethyl chitosan and CA;[28,29] also, antibacterial properties of cyanoethylchitosan/CA polymer blended membrane has been improved.[27]

It has been demonstrated that the existence of inorganic segments could enhance the chemical stability, thermal tolerance, and mechanical properties, and tune the microstructure and

Additional Supporting Information may be found in the online version of this article.

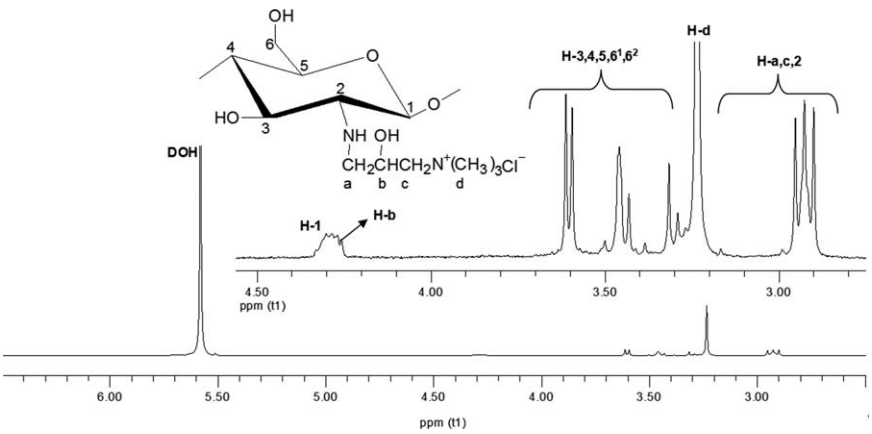


**Figure 1.** $^1$H-NMR spectrum for HTCC in $D_2O/CF_3COOD$.

hydrophilic–hydrophobic balance of membranes.[30,31] To date, a variety of inorganic nanoparticles, such as $SiO_2$, ZnO, $Al_2O_3$, $Fe_3O_4$, and $TiO_2$, have been introduced into polymer matrix to afford the polymer/inorganic nanoparticles composite materials.[32–34] Among these inorganic substances, $TiO_2$ shows good stability, resisting and decomposing bacteria, hydrophilicity, and UV resistance.[35–38] Currently, the polymer–inorganic composite membranes are fabricated by *in situ* sol–gel method and blending.[39] However, too fast of a sol–gel reaction rate will generate inorganic particles with poor uniformity and controllability during membrane fabrication.[30,40] As a result, $TiO_2$ nanoparticles often easily aggregate to large irregular shape in membrane casting solution, which leads to the generation of many nonselective voids at the polymer/$TiO_2$ interface.[41,42] Because CTS and its derivatives have excellent biocompatibility and film-forming ability, it is expected to obtain better dispersing performance by blending the CTS-based polymer with $TiO_2$ nanoparticles.

Although CTS has been chosen as a blend polymer to improve the properties of the CA membrane by introducing reactive sites into the membrane material and to reduce the aggregation of $TiO_2$ nanoparticles, CTS still has some shortcomings. Especially, it is only dissolved in acid solutions so that its physical structure and mechanical strength will be affected. Herein, we used *N*-[(2-hydroxy-3-trimethylamonium) propyl] chitosan (HTCC) to solve this problem. HTCC is one type of quaternary CTS with good water solubility, moisture retentiveness, antibacterial activity, mucoadhesivity, and permeability-enhancing property because of hydration and strong steric hindrance of positively charged quaternary amino groups. However, to the best of our knowledge, there is no report on the blend membranes of CA and HTCC and nano-$TiO_2$. Particularly, the mechanical strength of the membrane was optimized by our method.

In this study, CTS was modified into HTCC by introducing quaternary ammonium groups grafted with $-NH_2$ groups. A series of HTCC/CA/$TiO_2$ nanocomposite membranes were prepared, and the reaction condition was optimized to get a better tensile strength. The composite membranes were characterized by Fourier transform infrared (FTIR) spectroscopy, X-ray diffraction (XRD), and thermogravimetric analysis (TGA). The mechanical strength, swelling properties, and antibacterial activities of the resulting membranes were investigated as well.

## EXPERIMENTAL

### Materials

CTS and CA were purchased from Sinopharm Chemical Reagent Co. (Shanghai, China). The molecular weight of CTS was $1.09 \times 10^6$ Da, and the deacetylation degree was 73.39%. Glycidyl trimethylammonium chloride (GTMAC) with a purity of 96% was purchased from Shandong Sangong Chemical Co. (Shandong, China) $TiO_2$ nanoparticles were kindly provided by Powder Center of Nanjing University of Science and Technology, China. Acetic acid ($CH_3COOH$), sodium hydroxide (NaOH), acetone, isopropanol, ethanol, and sodium chloride were purchased from Sinopharm Chemical Reagent Co. and were used directly without further purification. Nutrient agar, beef extract, and polypeptone (Sinopharm Chemical Reagent Co.) were used for the antibacterial activity test.

### *Preparation of HTCC/CA/$TiO_2$ Membranes*

Two grams of CTS was dissolved in 100 mL of 2 wt % acetic acid solution. Then, the solution was adjusted with 1*M* NaOH solution to pH = 9 and kept stirring for 2 h to allow alkalinization. The precipitate obtained was dissolved in isopropanol, and the solution was stirred at 60°C for 4 h, to which 15 wt % aqueous solution of GTMAC was added dropwise. After stirring at 80°C for 8 h, the clear viscous solution was cooled to ambient temperature and poured into acetone. The reaction mixture was filtered, and the precipitate was washed three times with acetone and dried at 80°C to obtain HTCC (for $^1$H-nuclear magnetic resonance (NMR) spectrum of CTS, see Supporting Information Figure S1). The $^1$H-NMR spectrum of HTCC is shown in Figure 1. The signals at 4.36, 2.94, 3.63, 3.59, 3.32, and 3.74 ppm were assigned to H-1, H-2, H-3, H-4, H-5, and H-6, respectively. The strong peak at 3.21 ppm corresponds to the methyl groups of the quaternary ammonium side chain ($-N^+(CH_3)_3$). The signals at 2.93, 4.30, and 3.04 ppm indicate the presence of H-a, H-b, and H-c, respectively.

HTCC and CA polymer solution were mixed in 2 wt % proportion (the casting solution) by using appropriate solvent acetic

acid aqueous solution, and then the solution was stirred at 50°C for 1 h to form a homogeneous polymer mixture. Afterward, $TiO_2$ was added quantitatively (0.5, 1.0, 1.5, and 2.0%) to the mixture and dispersed evenly by continuous stirring and ultrasonic treatment. After degassing, the resulting homogeneous mixture was transferred into acrylic petri dishes and dried at 60°C to form the HTCC/CA/$TiO_2$ composite membranes. The membranes were finally washed with 0.1*M* NaOH for 1 h to completely remove all residual acid. Then, the membranes were thoroughly washed with deionized water until a neutral pH was obtained, and then naturally dried at room temperature.

### Mechanical Properties

Mechanical properties, i.e., tensile strength and elongation-at-break, of the prepared sample membranes were measured using Universal Testing Machine (AGS-S, Shimadzu, Japan) following the ASTM-D6693-01 standard method. Membranes with a gauge length of 45 mm and width of 5 mm were stretched at an extension speed of 2 mm $min^{-1}$ at 25°C. The resulting data were taken from the average of at least three samples.

### Swelling Properties

The swelling properties of the membranes were tested as described: membrane of appropriate size was immersed completely in deionized water for more than 24 h until equilibrium was reached, and the membrane was weighed followed by mopping it with blotting paper quickly. The wet membrane was then dried in the oven at 80°C until a constant weight was obtained.[43] The swelling degree (SD) of the membrane was calculated by the following equation:

$$\mathrm{SD}=\frac{M_w-M_d}{M_d}\times 100\% \quad (1)$$

where, $M_w$ and $M_d$ are the weights of the wet and dry membranes, respectively.

### Antibacterial Activity Test

Antibacterial activity test was carried out using agar disk diffusion method according to the National Committee for Clinical Laboratory Standards (NCCLS).[44] The inhibition zone assay on culture medium was used to determine the antibacterial ability of obtained membranes against *Escherichia coli* (*Rosetta* and *DH5α*) and *Bacillus subtilis*, which were provided by the Department of Biological Engineering, Nanjing University of Science and Technology (Nanjing, China).

### Characterization of the Membranes

The $^1$H-NMR spectrum of HTCC was recorded on a JEOL spectrometer (EX270) using $D_2O/CF_3COOD$ (v/v = 95 : 5) as the solvent.

The attenuated total reflectance-FTIR spectra of CTS-based membranes were performed on an FT-IR spectrophotometry equipment (IR Prestige-21, Shimadzu), with a spectral range from 4000 to 400 $cm^{-1}$. The crystallinities of membranes were analyzed by XRD with CuKα X-ray diffractometer (D8 Advance, Bruker Co., Germany) at 25°C.

XRD patterns were recorded in an angular range of 10°–80° (2$\theta$), at a scanning rate of 10° $min^{-1}$. Thermal degradation and stability of the CTS-based membranes were measured by thermal gravimetric analyzer (TG, STA409PC) under nitrogen atmosphere between 50°C and 700°C at a 10°C $min^{-1}$ increment rate. Nitrogen gas was utilized for flushing purpose, at the rate of 20 mL/$min^{-1}$.

The morphology of membranes was studied using scanning electron microscopy (SEM; JEOL JSM-6380LV). Prior to SEM observation, the membranes were frozen and fractured in liquid nitrogen, using double-sided adhesive tape and coated with gold under vacuum. Atomic force microscopy (AFM) images of these films were obtained using multimode nanoscope IV (Bruker Co.) operated in tapping mode.

## RESULTS AND DISCUSSION

### Tensile Strength Optimization of Membrane

Figure 2 shows the tensile strength of membranes with the changes in acetic acid concentration, temperature, $n_{CTS}$ : $n_{GTMAC}$, and CA content. Because of the insolubility of CA in dilute acid, high concentration of acetic acid aqueous solution was needed as the solvent. During the experiments, the maximum tensile strength value was achieved in 70% acetic acid. In 60% acetic acid or below, CA could not dissolve entirely; whereas in 80% or above, the solubility of HTCC was limited, and its degradation was accelerated. We also found that the mechanical strength of membrane improved when the CA content increases. We also found that the mechanical strength of membrane improved when the CA content increases. However, when the CA content reaches above 60%, precipitation will appear on the surface of membrane, which possibly resulted in the unreasonable mixing apportion of two polymers. Furthermore, as seen in Figure 2, when the mole ratio of CTS to GTMAC is 2 : 1, the tensile strength reaches maximum at 60°C. However, it should be noted that, with the decreased amount of quaternary ammonium compounds, the grafting quantity reduced correspondingly. Because of the very similar results, a molar ratio of CTS/GTMAC of 1 : 1 could be selected. Thus, we got the optimum preparation conditions: acetic acid concentration 70%, mass fraction of CA 50%, CTS/GTMAC mole ratio 1 : 1, and drying temperature 60°C.

### Mechanical Properties

The tensile strength and elongation-at-break of CTS-based membranes are shown in Table I. The HTCC/CA membrane showed much greater maximum strain than the HTCC membrane, mainly due to the poorer strength of HTCC itself compared with CA. As $TiO_2$ was added, the tensile strength and elongation-at-break of HTCC/CA/$TiO_2$ composite membrane increased at first and then decreased, and the maximum values were achieved at 1.0 wt % $TiO_2$ content. The better mechanical performance of membranes might be attributed to the production of hydrogen and Ti-O bonds between $TiO_2$ and polymers. Lee *et al.*[45] found that after the incorporation of $TiO_2$ particles, all of the elongation-at-break values were higher than that of PVDF/PMMA blend. Enhancement in the values was probably because some $TiO_2$ particles functioned as physical junctions in the films during extrusion.[45] Tao *et al.*[46] confirmed the result. However, excess nano-$TiO_2$ particles are difficult to disperse in membrane casting solution evenly. Together with the strong aggregation effect for nano-$TiO_2$ particles, the molecular

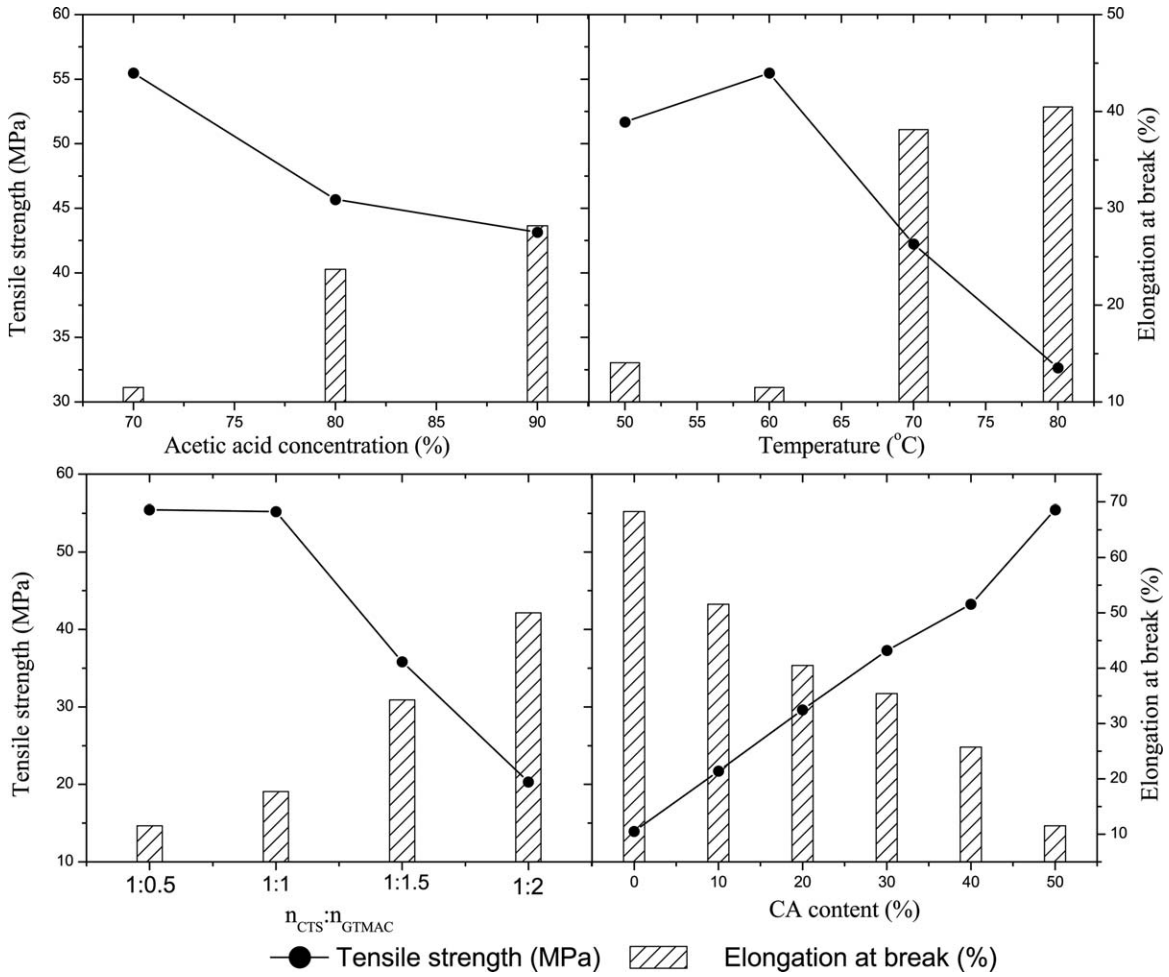


**Figure 2.** Tensile strength values of membranes with the changes of acetic acid concentration (a), temperature (b), $n_{CTS}$ : $n_{GTMAC}$ (c), and CA content (d).

interaction of membranes and the arrangement of polymer chains will be disturbed seriously through steric effect, leading to weak mechanical performance.

**Table I.** Mechanical Properties, Swelling Degree, and Ion Exchange Capacity of CTS, HTCC, HTCC/CA, and HTCC/CA/$TiO_2$ Membranes

| Membrane code | Tensile strength (MPa) | Elongation-at-break (%) | SD (%) |
|---|---|---|---|
| CTS | 25.79 | 59.63 | 249.61 |
| HTCC | 13.95 | 68.34 | 375.45 |
| HTCC/CA | 55.21 | 37.69 | 123.25 |
| HTCC/CA + 0.5 wt % $TiO_2$ | 59.69 | 41.43 | 109.05 |
| HTCC/CA + 1.0 wt % $TiO_2$ | 84.29 | 55.12 | 101.36 |
| HTCC/CA + 1.5 wt % $TiO_2$ | 63.86 | 49.11 | 122.83 |
| HTCC/CA + 2.0 wt % $TiO_2$ | 46.17 | 42.11 | 166.54 |

**Swelling Properties**

Swelling ability is another important property for the practical applications of CTS-based membranes. As shown in Table I, the SD of HTCC was higher than that of pure CTS, mainly because the —$NH_2$ group of CTS was grafted by stronger hydrophilic group —$CH_2CH(OH)CH_2N(CH_3)_3^+$. The addition of CA significantly reduced the SD of membranes, even below that of CT because of the poorer water adsorption capacity of CA. With the introduction of nano-$TiO_2$ particles, it was found that the SD of membranes decreased to a minimum value when $TiO_2$ content increased up to 1.0 wt %. This might be attributed to the strong interaction between polar $TiO_2$ molecules and the abundance of —OH groups of the polymer. Herein, the generation of new chemical bond Ti-O blocked the hydrogen bonding of —OH group with $H_2O$ molecules, and so the water uptake was reduced. However, the SD of HTCC/CA/$TiO_2$ began to increase significantly when $TiO_2$ content exceeded 1.0 wt %. The possible reason is that water molecules were absorbed by the $TiO_2$ particles on the composite membrane and polarized to form —OH groups. Furthermore, excess $TiO_2$ nanoparticles markedly interfered with the ordered packing of polymer chains by steric effect, which provided space for the existence of $H_2O$ molecules.

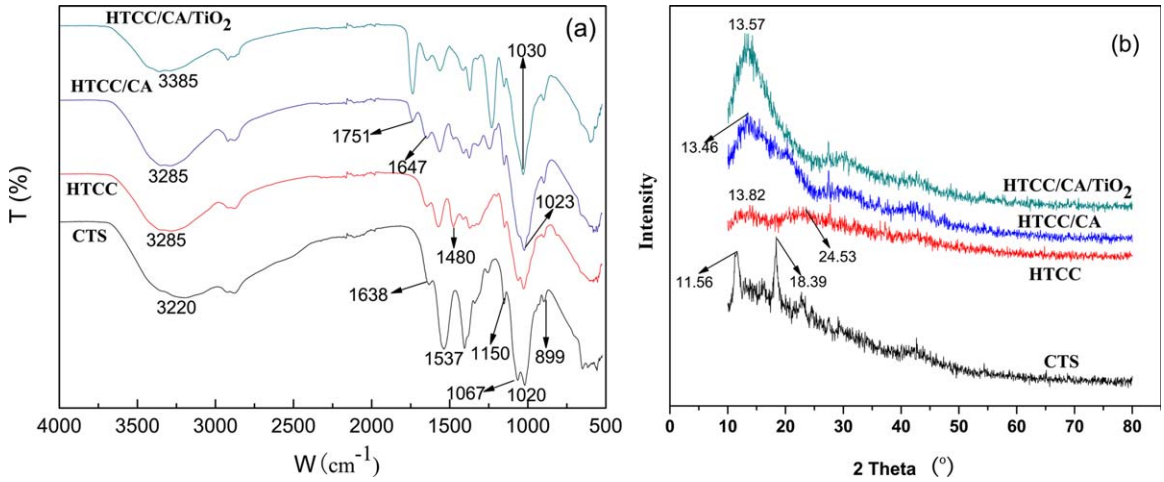


**Figure 3.** FTIR (a) and X-ray diffractograms (b) of pure CTS membrane, HTCC membrane, HTCC/CA membrane, and HTCC/CA/$TiO_2$ membrane. [Color figure can be viewed in the online issue, which is available at wileyonlinelibrary.com.]

### Attenuated Total Reflectance-FTIR Analysis

The IR spectrum of HTCC is shown in Figure 3(a). We can see that there is a slight shift but little change of the characteristic absorption peaks of $\beta$-glycosidic bond at 1150 and 899 $cm^{-1}$ between the four kinds of membranes, which indicates that $\beta$-glycosidic bond did not participate in the process of film forming, and the heterocycle of CTS is still keeping its original structure. In the IR spectrum of CTS membrane, there is a stretching vibration peak of —OH at 3220 $cm^{-1}$, which is also affected by N—H stretching vibration, a symmetric stretching peak of —$CH_2$— at 2900 $cm^{-1}$, and 2 C—O absorption peaks of $C_3$ and $C_6$ on CTS chains at 1067 and 1012 $cm^{-1}$. Compared with the IR spectrum of HTCC membrane to CTS, the stretching vibration peak of —OH and N—H shifts from 3220 to 3285 $cm^{-1}$, the half peak width widen because of an increase in the number of —OH, and a new —$CH_3$ stretching vibration peak appears at 1480 $cm^{-1}$, which proves the introduction of quaternary amino groups at the —$NH_2$ sites on the CTS chains.

When comparing the IR spectrum of HTCC/CA membrane with that of HTCC, it was found that a new absorption peak of C═O on CA chains appears at 1751 $cm^{-1}$, but the C—O peak of $C_3$ at 1067 $cm^{-1}$ weakened sharply, which may be due to the strong hydrogen bonding between CA and HTCC molecules, showing good compatibility and miscibility between CA and HTCC. In the IR spectrum of HTCC/CA/$TiO_2$ membrane, the peak of —OH and N—H shifts to 3385 $cm^{-1}$ and becomes wider, the C—O peak disappears completely, and a slight shift occurs compared with that of HTCC/CA membrane, which may be caused by the formation of Ti...OH between $TiO_2$ and —OH, and it is good for the dispersal of $TiO_2$ nanoparticles in membrane.

### XRD Analysis

According to Figure 3(b), the main diffraction peaks of CTS appear at 11.56° and 18.39°, for a mixture of two crystalline forms. Compared with the XRD pattern of CTS membrane, there are two wide and blunt diffraction peaks at 13.82° and 24.53° of HTCC. It is possibly because the introduction of quaternary amino groups at the —$NH_2$ sites on the CTS chains damaged the formation of hydrogen bonding between —$NH_2$ and —OH and disturbed the orderly arrangement of CTS chain, leading to the reduced crystallinity. Compared with HTCC, the main diffraction peak of HTCC/CA appears at 13.46°, but that of HTCC is not obvious, showing that the structure of CA changes little, but HTCC almost does not form crystalline region during the film-forming process. This means that there exists a good compatibility and miscibility between CA and HTCC. There are no characteristic absorption peaks of nano-$TiO_2$ at 25°, 38°, and 49° in the XRD pattern of HTCC/CA/$TiO_2$,[47] indicating that the $TiO_2$ nanoparticles could be in amorphous states or crystalline-phase $TiO_2$ was not detected. One of the reason is that the amount of $TiO_2$ is too low to be detected by XRD. The other reasons may be the complete dispersion in HTCC, presumably due to the wrapped $TiO_2$ in the HTCC membrane. However, the existence of $TiO_2$ nanoparticles would disturb the orderly arrangement of the polymer chains through space interval and the formation of hydrogen bonding, leading to the decrease in the membrane crystallinity.[46,48]

### Thermogravimetric Analysis

The results of TGA of CTS, HTCC, HTCC/CA, and HTCC/CA/$TiO_2$ membranes are illustrated in Figure 4. The pure CTS membrane thermal degradation consists of two stages. The first stage is weight loss of up to 8.10% with a maximum rate at 100°C; this temperature is related to the evaporation of water present in the sample. The second stage starts at 150°C with maximum at 298°C corresponding to a weight loss of 51.35%, which is assigned to the depolymerization of CTS chains. This degradation process is in agreement with the results of CTS degradation as reported.[49] Compared with CTS membrane, the mass change of first stage of HTCC membrane is less, and the second stage starts ahead at 175°C, with maximum at 288°C, corresponding to weight loss of 55.1%. This phenomenon may be explained by the interaction between CTS and GTMAC, which disturbs the ordered packing of CTS intermolecular chains and also confirmed the results of XRD patterns. The HTCC/CA membrane shows a two-stage thermal degradation as well. The first stage is similar to that of CTS membrane, but in

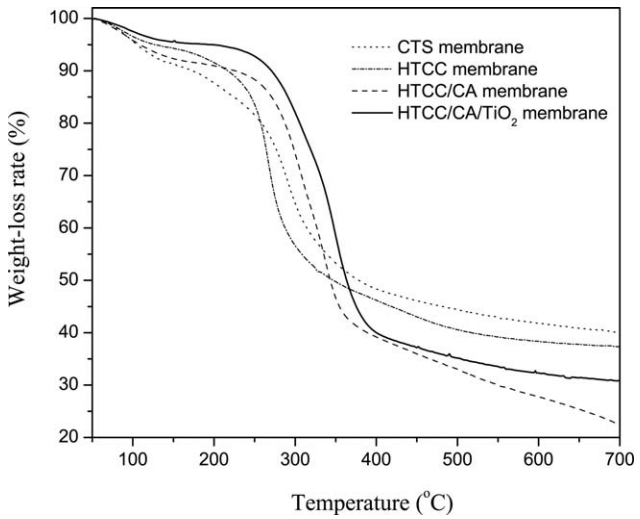


**Figure 4.** Thermogravimetric analysis of CTS, HTCC, HTCC/CA, and HTCC/CA/$TiO_2$ membranes.

the second stage, about 68.83% of membrane mass is lost, with maximum at a delayed temperature of 330°C, indicating that the thermal stability of the blend membrane improved significantly with the addition of CA. It could be because that the interaction between HTCC and CA increases the rigidity of polymer chains and enhances the energy of breaking down the polymer chains. This interaction is due to the covalent bonds between HTCC and CA chains. The TGA results also confirmed the good compatibility and mixability between HTCC and CA in the blends. In the TG curves of HTCC/CA/$TiO_2$ composite membranes, the second stage changed apparently. Furthermore, the weight loss of the membrane was reduced, and the decomposition temperature was increased with the introduction of $TiO_2$, corresponding to the enhanced thermal stability of composite membranes. The results also confirmed that $TiO_2$ nanoparticles were dispersed uniformly in the membrane structure and had a good compatibility with HTCC and CA. It is probably due to the formation of Ti-O bonds in the blends, and the surface hydroxyl group can also form a hydrogen bond with the polymer molecules.

### Surface Morphology by SEM and AFM

SEM photographs for the surface and the cross-sectional views of the HTCC/CA/$TiO_2$ membrane are shown in Figure 5. Within the detection limit of the SEM, the surface of the composite membrane is smooth, and the cross-sectional view of the composite membrane shows that there are no obvious aggregate, phase separation phenomena, and the structure is compact. These results indicate that HTCC molecules have a good compatibility with CA and that nano-$TiO_2$ can be well dispersed in the HTCC matrix.

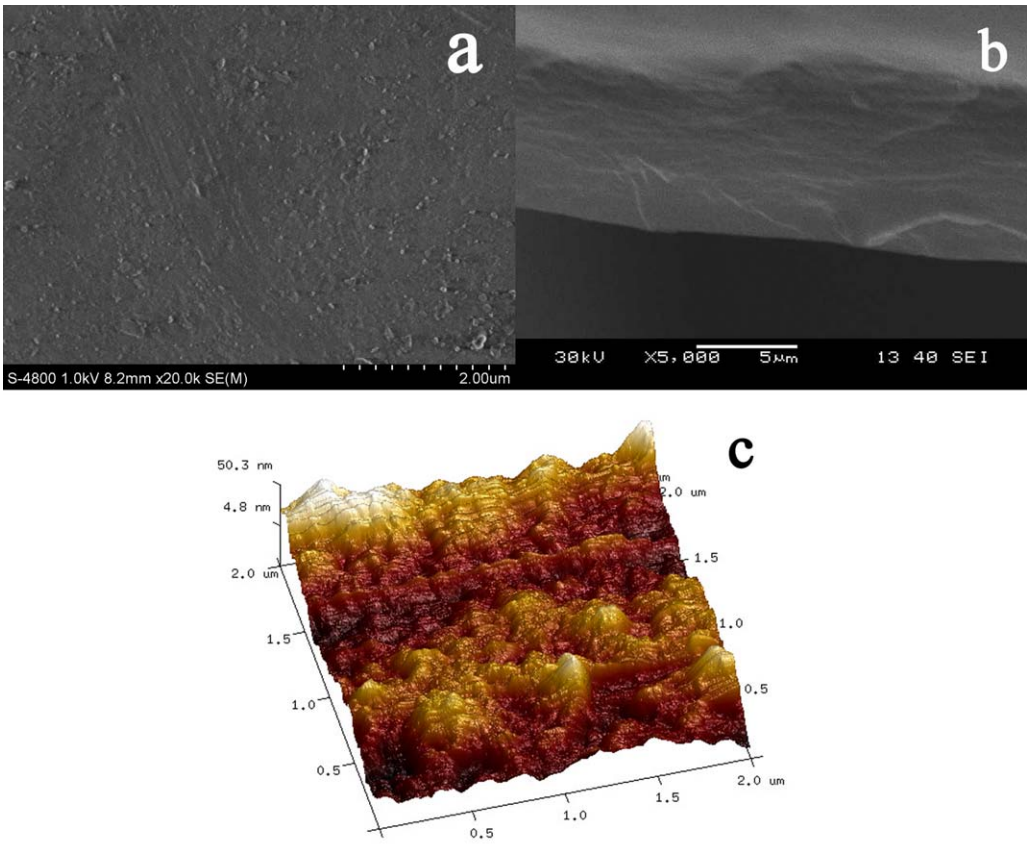


**Figure 5.** Surface SEM image (a), cross-sectional SEM image (b), and three-dimensional AFM topographic image (c) of HTCC/CA/$TiO_2$ membrane. [Color figure can be viewed in the online issue, which is available at wileyonlinelibrary.com.]

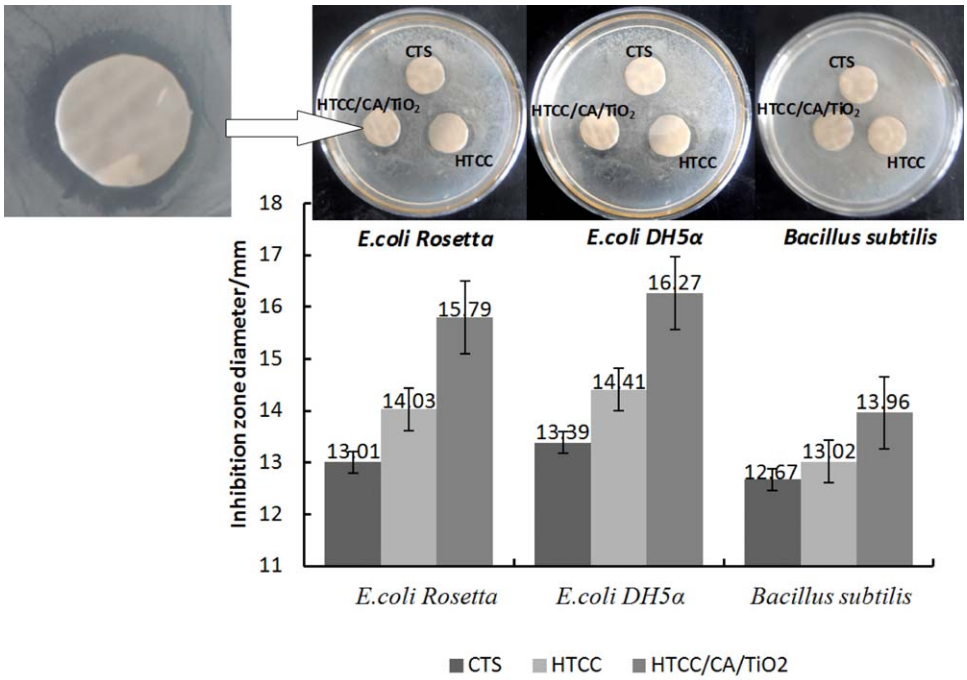


**Figure 6.** Representative images and diameter of inhibiting bacteria circle of pure CTS, HTCC, and HTCC/CA/$TiO_2$ membranes against Gram-negative *E. coli* (*Rosetta* and *DH5α*) and Gram-positive *Bacillus subtilis*. [Color figure can be viewed in the online issue, which is available at wileyonlinelibrary.com.]

Moreover, AFM image can yield more information on the membrane surface. Figure 5(b) shows the 3-D AFM images of the prepared HTCC/CA/$TiO_2$ composite membrane, which are presented in (2 $\mu$m × 2 $\mu$m) scanning area. It can be seen that the surface of the membranes is uneven (not smooth), which consists of a mass of peaks and small crater–valley-type structures with the mean roughness ($R_a$) = 9.56 nm and the root mean square roughness ($R_q$) = 11.9 nm. Obviously, the membrane roughness reflects the surface porosity because the crater–valleys have been verified as the pores on the surface.

### Antibacterial Activity

The inhibitory activity of CTS-based membranes was studied by an inhibition zone of bacterial growth around the circular membrane disk. The result is presented in Figure 6. The result demonstrates that all the composite membranes could inhibit the bacterial growth. It is observed that HTCC/CA/$TiO_2$ membranes exhibited better antibacterial performance toward *E. coli* (*DH5α* and *Rosetta*) than toward *B. subtilis*, and the inhibition zones of *E. coli DH5α* growth is close to that of *E. coli Rosetta* growth. For the Gram-negative bacterium *E. coli*, the cell wall is made up of a thin layer of peptidoglycan with low cross-linking density and has flagella outside;[50] so the membranes could easily adsorb *E. coli* and showed stronger antimicrobial activity against *E. coli*. However, the cell wall of the Gram-positive bacterium *B. subtilis* is composed of thick layers of peptidoglycan with high cross-linking degree, which restricts the formation of a double molecule layer structure to interact with the cationic polymers.[51,52] Hence, the antibacterial activity of these membranes was stronger against *E. coli* than *B. subtilis*, which was attributed to the different cellular structures of bacteria.

One the other hand, as seen from Figure 6, the inhibition zone diameters of HTCC membranes toward *E. coli DH5α* and *Rosetta* and *B. subtilis* were 14.03, 14.41, and 13.02 mm, respectively. It was illustrated that the antibacterial activity of HTCC membranes was stronger than that of CTS membrane. This could be explained by the substitution of —$NH_2$ groups by —$CH_2CH(OH)CH_2N(CH_3)_3^+$, which is more electropositive than —$NH_3^+$ and made it easier to absorb Gram-negative bacteria. Additionally, it was observed that the inhibition zone diameters of HTCC/CA/$TiO_2$ membranes toward *E. coli DH5α* and *Rosetta* and *B. subtilis* were 15.79, 16.27, and 13.96 mm, respectively. It is clear that the antibacterial effect of HTCC/CA/$TiO_2$ membranes increased much more than that of HTCC membrane. It is reported that anatase $TiO_2$ film exhibits a strong photocatalytic reaction under UVA illumination and the bactericidal activity of $TiO_2$ is directly related to ultraviolet light absorption and the formation of various reactive species, such as superoxide radicals and hydroxyl radicals.[53,54] In our study, although the antibacterial tests were carried out under the visible light, HTCC/CA/$TiO_2$ membranes were preprocessed under the 16 W UV lamp for 30 min. One purpose is for sterilization, which can eliminate the bacterial interference on the membrane surface. The other purpose is that the electron-hole pairs on $TiO_2$ could be produced to form strong oxidizing free radicals under ultraviolet radiation. As expected, the higher antibacterial activity of HTCC/CA/$TiO_2$ membranes is due to the synergistic antibacterial effects of the introduction of stronger cationic group and the photocatalytic reaction of the $TiO_2$ coating.

## CONCLUSIONS

We have successfully prepared a new kind of HTCC/CA/$TiO_2$ composite membrane by blending two polymers HTCC and

CA, with $TiO_2$ as the introduced inorganic component. This membrane bears enhanced mechanical strength, thermal stability, and lowered water uptake. To improve tensile strength of the membranes, we optimized the blending reaction conditions, such as acetic acid concentration, temperature, ratio of $n_{CTS}$ : $n_{GTMAC}$ and the CA content. Our result showed that the dispersion of nano-$TiO_2$ particles into the HTCC/CA membrane not only increased its mechanical properties but also enhanced its antibacterial activities. The antibacterial properties of the membranes were compared to elucidate the significance of stronger cationic group and the existence of nano-$TiO_2$ particles, which have synergistic effect on improving antibacterial activity against Gram-negative *E. coli* (*Rosetta* and *DH5α*) and Gram-positive *B. subtilis*. Our method is helpful to extend the application of CTS-based membranes in many areas, such as food packaging, biomedical materials, etc.

## ACKNOWLEDGMENTS

This work was financially supported by National Natural Science Foundation of China (grant no. 51208259) and the Jiangsu Key Laboratory of Chemical Pollution Control and Resources Reuse, Nanjing University of Science and Technology (grant no. 30920140122008).

## REFERENCES

1. Salehi, E.; Madaeni, S.; Rajabi, L.; Vatanpour, V.; Derakhshan, A.; Zinadini, S.; Ghorabi, S.; Ahmadi, M. H. *Sep. Purif. Technol.* **2012**, *89*, 309.
2. Zhang, W.; Li, G.; Fang, Y.; Wang, X. *J. Membr. Sci.* **2007**, *295*, 130.
3. Chen, J. H.; Liu, Q. L.; Zhang, X. H.; Zhang, Q. G. *J. Membr. Sci.* **2007**, *292*, 125.
4. Choudhari, S. K.; Kittur, A. A.; Kulkarni, S. S.; Kariduraganavar, M. Y. *J. Membr. Sci.* **2007**, *302*, 197.
5. Clasen, C.; Wilhelms, T.; Kulicke, W. M. *Biomacromolecules* **2006**, *7*, 3210.
6. Tripathi, B. P.; Kumar, M.; Saxena, A.; Shahi, V. K. *J. Colloid Interface Sci.* **2010**, *346*, 54.
7. Yu, Q.; Song, Y.; Shi, X.; Xu, C.; Bin, Y. *Carbohydr. Polym.* **2011**, *84*, 465.
8. Zhang, Q. G.; Liu, Q. L.; Zhu, A. M.; Xiong, Y.; Ren, L. *J. Membr. Sci.* **2009**, *335*, 68.
9. Yang, J. M.; Chiu, H. C. *J. Membr. Sci.* **2012**, *419*, 65.
10. Huang, R.; Chen, G.; Yang, B.; Gao, C. *J. Appl. Polym. Sci.* **2010**, *118*, 2358.
11. Zhao, Z.; Zheng, J.; Wang, M.; Zhang, H.; Han, C. C. *J. Membr. Sci.* **2012**, *394*, 209.
12. Khayet, M.; Villaluenga, J.; Valentin, J.; López-Manchado, M.; Mengual, J.; Seoane, B. *Polymer* **2005**, *46*, 9881.
13. Tripathi, B. P.; Saxena, A.; Shahi, V. K. *J. Membr. Sci.* **2008**, *318*, 288.
14. Wang, Y.; Zhang, Q.; Zhang, C.; Li, P. *Food Chem.* **2012**, *132*, 419.
15. Pandey, R. P.; Shahi, V. K. *J. Membr. Sci.* **2013**, *444*, 116.
16. Liu, C. X.; Bai, R. B. *J. Membr. Sci.* **2006**, *284*, 313.
17. Lu, L. Y.; Peng, F. B.; Jiang, Z. Y.; Wang, J. H. *J. Appl. Polym. Sci.* **2006**, *101*, 167.
18. Svang-Ariyaskul, A.; Huang, R. Y. M.; Douglas, P. L.; Pal, R.; Feng, X.; Chen, P.; Liu, L. *J. Membr. Sci.* **2006**, *280*, 815.
19. Devi, D. A.; Smitha, B.; Sridhar, S.; Aminabhavi, T. M. *J. Membr. Sci.* **2006**, *280*, 138.
20. Rao, K. S. V. K.; Subha, M. C. S.; Sairam, M.; Mallikarjuna, N. N.; Aminabhavi, T. M. *J. Appl. Polym. Sci.* **2007**, *103*, 1918.
21. Shenvi, S.; Ismail, A. F.; Isloor, A. M. *Ind. Eng. Chem. Res.* **2014**, *53*, 13820.
22. Abedini, R.; Mousavi, S. M.; Aminzadeh, R. *Desalination* **2011**, *277*, 40.
23. Gaurav, A.; Ashamol, A.; Deepthi, M.; Sailaja, R. *J. Appl. Polym. Sci.* **2012**, *125*, E16.
24. Jayalakshmi, A.; Rajesh, S.; Senthilkumar, S.; Sankar, H. S. H.; Mohan, D. *J. Ind. Eng. Chem.* **2014**, *20*, 133.
25. Isogai, A.; Atalla, R. *Carbohydr. Polym.* **1992**, *19*, 25.
26. Liu, X.; Chen, Q.; Pan, H. *J. Mater. Sci.* **2007**, *42*, 6510.
27. Abou-Zeid, N.; Waly, A.; Kandile, N.; Rushdy, A.; El-Sheikh, M.; Ibrahim, H. *Carbohydr. Polym.* **2011**, *84*, 223.
28. Boricha, A. G.; Murthy, Z. V. P. *Chem. Eng. J.* **2010**, *157*, 393.
29. Boricha, A. G.; Murthy, Z. V. P. *J. Polym. Eng.* **2011**, *31*, 333.
30. Yang, D.; Li, J.; Jiang, Z.; Lu, L.; Chen, X. *Chem. Eng. Sci.* **2009**, *64*, 3130.
31. Emadzadeh, D.; Lau, W. J.; Matsuura, T.; Rahbari-Sisakht, M.; Ismail, A. F. *Chem. Eng. J.* **2014**, *237*, 70.
32. Li, L.; Deng, J.; Deng, H.; Liu, Z.; Xin, L. *Carbohydr. Res.* **2010**, *345*, 994.
33. Shen, J.; Xi, J.; Zhu, W.; Chen, L.; Qiu, X. *J. Power Sources* **2006**, *159*, 894.
34. Jian, P.; Yahui, H.; Yang, W.; Linlin, L. *J. Membr. Sci.* **2006**, *284*, 9.
35. Chen, X.; Mao, S. S. *Chem. Rev.* **2007**, *107*, 2891.
36. Shi, F.; Ma, Y.; Ma, J.; Wang, P.; Sun, W. *J. Membr. Sci.* **2012**, *389*, 522.
37. Wu, Z.; Sun, G.; Jin, W.; Hou, H.; Wang, S.; Xin, Q. *J. Membr. Sci.* **2008**, *313*, 336.
38. Huang, X.; Deng, J.; Xu, L.; Shen, P.; Zhao, B.; Tan, S. *Acta Chim. Sin.* **2012**, *70*, 1604.
39. Kariduraganavar, M. Y.; Kulkarni, S. S.; Kittur, A. A. *J. Membr. Sci.* **2005**, *246*, 83.
40. Zhao, J.; Wang, F.; Pan, F.; Zhang, M.; Yang, X.; Li, P.; Jiang, Z.; Zhang, P.; Cao, X.; Wang, B. *J. Membr. Sci.* **2013**, *446*, 395.
41. Hojjati, B.; Sui, R.; Charpentier, P. A. *Polymer* **2007**, *48*, 5850.
42. Li, J.; Zhu, L.; Wu, Y.; Harima, Y.; Zhang, A.; Tang, H. *Polymer* **2006**, *47*, 7361.

43. Sivakumar, M.; Mohanasundaram, A. K.; Mohan, D.; Balu, K.; Rangarajan, R. *J. Appl. Polym. Sci.* **1998**, *67*, 1939.
44. National Committee for Laboratory Standards. Performance Standards for Antimicrobial Disk Susceptibility Tests. Approved Standard M2-A8; NCCLS: Wayne, PA, **2003**.
45. Lee, J. G.; Kim, S. H.; Kang, H. C.; Park, S. H. *Macromol. Res.* **2013**, *21*, 349.
46. Tao, Y.; Pan, J.; Yan, S.; Tang, B.; Zhu, L. *Mater. Sci. Eng. B* **2007**, *138*, 84.
47. Chen, X.; Yang, H.; Gu, Z.; Shao, Z. *J. Appl. Polym. Sci.* **2001**, *79*, 1144.
48. Yang, D.; Li, J.; Jiang, Z.; Lu, L.; Chen, X. *Chem. Eng. Sci.* **2009**, *64*, 3130.
49. Guinesi, L. S.; Cavalheiro, É. T. G. *Thermochim. Acta* **2006**, *444*, 128.
50. Liu, H.; Du, Y.; Wang, X.; Sun, L. *Int. J. Food Microbiol.* **2004**, *95*, 147.
51. Kucerka, N.; Papp-Szabo, E.; Nieh, M. P.; Harroun, T. A.; Schooling, S. R.; Pencer, J.; Nicholson, E. A.; Beveridge, T. J.; Katsaras, J. *J. Phys. Chem. B* **2008**, *112*, 8057.
52. Liu, X.; Qi, S.; Li, Y.; Yang, L.; Cao, B. *Water Res.* **2013**, *47*, 3081.
53. Sunada, K.; Kikuchi, Y.; Hashimoto, K.; Fujishima, A. *Environ. Sci. Technol.* **1998**, *32*, 726.
54. Fu, G. F.; Vary, P. S.; Lin, C. T. *J. Phys. Chem. B* **2005**, *109*, 8889.